Anuário do Instituto de Geociências - UFRJ
www.anuario.igeo.ufrj.br

Mechanics of Cosserat Generalized Continuum and Modelling in Structural Geology

Mecânica do Contínuo Generalizado de Cosserat e Modelagem em Geologia Estrutural

Anderson Moraes[1]; Rodrigo P. de Figueiredo[2] & Eurípedes do A. Vargas Jr[3,4]

[1]Petróleo Brasileiro S.A., CENPES, Av. Horácio de Macedo, 950, 21941-915, Rio de Janeiro, RJ, Brasil
[2]Universidade Federal de Ouro Preto, Escola de Minas,
Departamento de Engenharia de Minas, Morro do Cruzeiro, s/n, 35400-000, Ouro Preto, MG, Brasil
[3]Universidade Federal do Rio de Janeiro, Instituto de Geociências, Departamento de Geologia,
Av. Athos da Silveira, 274, 21949-900, Rio de Janeiro, RJ, Brasil
[4]Pontifícia Universidade Católica do Rio de Janeiro, Departamento de Engenharia Civil,
Rua Marquês de São Vicente, 225, 22451-900, Rio de Janeiro, RJ, Brasil
E-mails: geologo_amoraes@uol.com.br; rpfigueiredo@yahoo.com.br; vargas@puc-rio.br
Recebido em: 30/08/2019 Aprovado em: 06/11/2019
DOI: http://dx.doi.org/10.11137/2020_1_366_375

Resumo

A concepção e interpretação de modelos em geologia estrutural, especialmente os numéricos, são eminentemente baseadas nos princípios da mecânica do contínuo clássico, onde a formulação intrínseca possui alto grau de simetria em sua própria essência. No entanto, as estruturas geológicas apresentam em todas as escalas de observação um nível notável de assimetria. Por outro lado, a mecânica do contínuo generalizado de Cosserat, ao incorporar comprimentos característicos da estrutura da matéria em suas leis constitutivas e em seus critérios de ruptura, conduz naturalmente à assimetria e à heterogeneidade dos campos cinemáticos e dinâmicos responsáveis pela estruturação presente em rochas. Baseado na formulação intrínseca dos meios contínuos de Cosserat, o presente trabalho enfatiza modelos conceituais, analíticos e numéricos que sugerem uma ampliação na interpretação da gênese e do desenvolvimento de estruturas geológicas, em particular as encontradas em zonas de falhas.
Palavras-Chave: Contínuo de Cosserat; Geologia Estrutural; Modelagem Numérica

Abstract

The conception and interpretation of models in structural geology, specially the numerical ones, are eminently based on the principles of classic continuum mechanics, where the intrinsic formulation has high degree of symmetry in its very essence. However, the geological structures carry in all scales a remarkable level of asymmetry. On the other hand, the mechanics of Cosserat generalized continuum, by incorporating characteristic lengths of the matter structure in its constitutive and strength laws, leads by itself to the asymmetry and the heterogeneity of the kinematic and dynamic fields responsible for rock fabric. Based on the intrinsic formulation of the Cosserat continuum, the present work emphasizes conceptual, analytical and numerical models that suggest the expansion in the interpretation of the genesis and development of geological structures, in particular those found in fault zones.
Keywords: Cosserat continuum; Structural Geology; Numerical Modelling

1 Introduction

Models in structural geology, being conceptual or coming from rock testing laboratory, from analogue experiments or, even more, from analytical and numerical methods, use the concepts of continuum mechanics in their design and particularly along the interpretation of their results. In particular, the recognition of the role of numerical modelling in structural geology has increased tremendously in recent decades mainly because of the possibility to test different concepts and physical conditions related to the development of geological structures in rocks. However, most of these models are based on the classic continuum mechanics.

In the classic continuum mechanics the stress and strain fields and the material physical properties are collapsed to points having three degrees of freedom for displacements in 3D. On the other hand, the mechanics of Cosserat generalized continuum, pioneered by the Cosserat brothers (Cosserat & Cosserat, 1909), incorporates finite lengths in microscale and, in addition to the three degrees of freedom for displacements, it allows three independent degrees of freedom for rotations. As this length with such properties is directly inserted in the mechanical formulation of a Cosserat continuum, asymmetries are generated for the stress and strain tensor fields, opening possibilities to improve the description of the mechanical behaviour of the materials, specially rocks in their different geological environments.

In the specific case of engineering, many works in the literature have dealt with the application of the generalized continuum mechanics, specially since the 1960s, although much less in comparison with works that use the classic continuum mechanics. Most of the works are devoted to the study of mechanical behaviour and strain localization in granular media, composite and fractal materials, soils and rocks (e.g. Mindlin, 1963; Sternberg & Muki, 1967; Besdo, 1985; Mühlhaus & Vardoulakis, 1987; Vardoulakis & Sulem, 1995; Adhikary *et al*., 1999; Tordesillas *et al.*, 2004; Tejchman, 2008; Khoei *et al*., 2010; Muller *et al*., 2011; Coetzee, 2014; Esin *et al*., 2017, Rattez *et al*., 2018; Ostoja-Starzewski *et al*., 2019). However, quite strange, in structural geology, a discipline that deals directly with the deformation of rocks, a granular material frequently structured by fractures in its essence, the number of works is still very small, being possibly pioneering the works of Biot (1965, 1967) on the mechanics of folding. In addition, studies can be highlighted on the general pattern of deformation in the processes of folding and faulting (Latham, 1985a,b; De Paor, 1994; Figueiredo, 1999; Mühlhaus *et al*., 2002; Bigoni & Gourgiotis, 2016), on the genesis of the inner structure in fault zones (Bauer & Tejchman, 1995; Figueiredo *et al*., 2004; Moraes, 2004; Veveakis *et al*., 2012; Zheng *et al*., 2016), on the mechanical interaction between blocks delimited by faults (Žalohar, 2012; Žalohar, 2015), on paleostress inversion from faults (Twiss *et al*., 1991, 1993; Twiss & Unruh, 1998; Žalohar & Vrabec, 2010) and on the understanding of earthquake seismology (Twiss & Unruh, 2007; Lee, 2011; Teisseyre, 2012; Žalohar, 2014; Žalohar, 2018).

The present work strives to strengthen the potential of the application of the mechanics of Cosserat generalized continuum in structural geology. Through the presentation of its basic formulation, it will be highlighted how simple models based on the mechanics of Cosserat generalized continuum may suggest the genesis and development of some geological structures, specifically those related to fault zones.

2 Background on the Mechanics of Cosserat Generalized Continuum

This section presents the basic formulation of the mechanics of Cosserat generalized continuum, regarding the main points addressed in this work. Further details on the mechanics of the generalized continuum media and their variants can be found in the classic work of Germain (1973) and also in Maugin (2017). Specifically, a comprehensive formulation on the mechanics of Cosserat generalized continuum is showed in Figueiredo *et al*. (2004).

Fundamentally, the mechanics of Cosserat generalized continuum, also called micropolar continuum mechanics, is a particularization of the mechanics of generalized continuum. In a Cosserat continuum, it is conceived the existence of rigid particles with finite lengths in microscale that suffers displacements and rigid rotations but do not deform (i.e., they do not change shape or volume), and these rotations are independent of the macroscale behaviour. In kinematic terms, being u'_i the microscale displacements (relative to the local coordinate system x'_i), u_i the macroscale displacements (relative to the global coordinate system x_i) and ω^c_{ij} the Cosserat micro-rotation tensor, we can write:

$$u'_i = u_i + \omega^c_{ij} x'_j \quad (1)$$

The indexes i and j range from 1 to 3 in 3D (1 to 2 in 2D). The first index refers to the unit normal vector acting on the face of the elementary unit of the continuum and the second index refers to the direction that que component acts. The relative displacement gradient tensor γ_{ij} is defined as:

$$\gamma_{ij} = \partial_j u_i - (\partial_j u'_i - \partial_i u'_j)/2 = \partial_j u_i - \omega^c_{ij} \quad (2)$$

Therefore, $\omega^c_{ij} = (\partial_j u'_i - \partial_i u'_j)/2$, where ∂_i represents the gradients in the i directions. One can divide γ_{ij} into its symmetric part, symbolized by indexes between ( ), and anti-symmetric part, symbolized by indexes between [ ], in the form:

$$\begin{aligned} \gamma_{(ij)} &= \varepsilon_{ij} \\ \gamma_{[ij]} &= \omega_{ij} - \omega^c_{ij} \end{aligned} \quad (3)$$

where ε_{ij} is the strain tensor in macroscale and ω_{ij} is the macroscale rotation tensor. Equation 3 is of fundamental importance for the mechanical implications of a Cosserat continuum. It is seen that the symmetric part of γ_{ij} coincides with the macrostrains, since there are no microscale strain, and the anti-symmetric part of γ_{ij} contains the rigid rotation difference between the macroscale and the microscale. As a result, it is seen that γ_{ij} is an asymmetric tensor. Additionally, the macroscopic gradient of the micro-rotations tensor k_{ijk} (unit of inverse of length) is defined as:

$$k_{ijk} = \partial_k \omega^c_{ij} \quad (4)$$

representing the curvatures along the continuous medium. Note that k_{ijk} is the gradient of ω^c_{ij}, and thus it is also an anti-symmetric tensor. Defining ω^c_i as the Cosserat micro-rotation vector (dual-vector of ω^c_{ij}) and k_i as the macroscopic gradient of the micro-rotations vector (dual-vector of k_{ijk}), from Equation 1 to Equation 4, we can write in 2D:

$$\begin{aligned} \gamma_{11} &= \partial_1 u_1 = \varepsilon_{11} \\ \gamma_{12} &= \partial_2 u_1 + \omega^c_3 \\ \gamma_{22} &= \partial_2 u_2 = \varepsilon_{22} \\ \gamma_{21} &= \partial_1 u_2 - \omega^c_3 \\ \kappa_1 &= \partial_1 \omega^c_3 \\ \kappa_2 &= \partial_2 \omega^c_3 \end{aligned} \quad (5)$$

In terms of stresses, as shown in Figueiredo *et al*. (2004), there are stress fields energetically related to the kinematic fields presented above. In this sense, the relative stress tensor τ_{ij} is directly related to the anti-symmetric tensor ω^c_{ij}, so that it is also an anti-symmetric tensor. Since σ_{ij} is the stress tensor of the classic continuum, the Cosserat stress tensor σ^c_{ij} is defined as:

$$\sigma^c_{ij} = \sigma_{ij} + \tau_{ij} \quad (6)$$

As a consequence, being the sum of a symmetric tensor with an anti-symmetric tensor, σ^c_{ij} is an asymmetric tensor. As a result, as shown in Figure 1 in 2D , the equilibrium conditions required for the Cosserat continuum arise from the emergence of moment (or couple) stresses m_i (unit of stress times length) applied to the arm dx'_j orthogonal to m_i in the elementary unit of the continuum. Thus, the moment stresses vectors m_1 and m_2 induce local momentum forces that balance the forces relative to the shear stresses σ^c_{12} and σ^c_{21} of the Cosserat stress tensor. In this way, the equilibrium equations for a Cosserat continuum in 2D are:

$$\begin{aligned} &\partial_1 \sigma^c_{11} + \partial_2 \sigma^c_{21} + \rho X_1 = 0 \\ &\partial_1 \sigma^c_{12} + \partial_2 \sigma^c_{22} + \rho X_2 = 0 \\ &\partial_1 m_1 + \partial_2 m_2 + (\sigma^c_{12} - \sigma^c_{21}) + \Theta \Rightarrow \partial_1 m_1 + \partial_2 m_2 + 2\sigma^a + \Theta = 0 \end{aligned} \quad (7)$$

where ρ is the density, X_i are volumetric forces, Θ is the volumetric moment and σ^a is the anti-symmetric shear stress given by:

$$\sigma^a = \frac{(\sigma_{12} - \sigma_{21})}{2} \quad (8)$$

representing at some extent a measure of the degree of asymmetry of σ^c_{ij}. In fact, by inspection of the last expression in Equation 7, it is clear that with the emergence of non-zero moment stresses gradients the shear components σ^c_{ij} and σ^c_{ji} of the Cosserat stress tensor are no longer necessarily equal, resulting, in general, in an asymmetric Cosserat stress tensor.

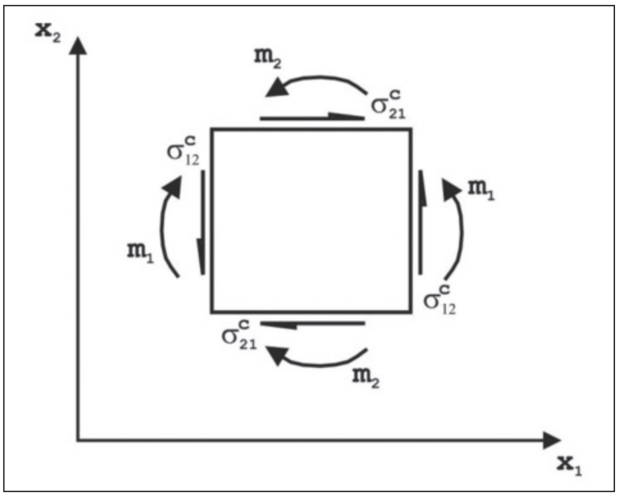

Figure 1 Representation in 2D of the cause of Cosserat stress tensor asymmetry. Moment stress vectors m_1 and m_2 induce local moment forces that equilibrate forces related to the different shear stresses σ^c_{12} and σ^c_{21} of the Cosserat stress tensor.

The kinematic and dynamic characteristics of the mechanics of Cosserat generalized continuum presented above make it possible to delineate constitutive relationships and flow criteria that are particularly important in structural geology. An isotropic elastic Cosserat continuum, as presented by Figueiredo *et al*. (2004) by slightly modifying the formulation of Teodorescu (1975), can be expressed by:

$$\sigma^c{}_{11} = \lambda\epsilon_{ij}\delta_{ij} + 2G\epsilon_{ij} + 2G_r\gamma_{[ij]}$$
$$m_i = B\kappa_i \qquad (9)$$

where δ_{ij} is the Kronecker delta (values of 1 for $i = j$ and 0 for $i \neq j$), λ and G are parameters analogous to the Lamé's parameters, G_r is the rotational modulus and B is the flexural modulus. The rotational modulus controls how much the microstructure influences the distribution of the macroscale stresses, being the parameter that couples the expressions of Equation 9. The relationship between the shear modulus G and the flexural modulus B has an interesting physical meaning. As suggested by Mindlin (1963) it is written:

$$l = \sqrt{\frac{B}{2G}} \qquad (10)$$

where l is the called characteristic length. The characteristic length may be regarded as the length of the microstructure of the medium. In this sense, the presence of characteristic lengths, a single one when is considered an isotropic medium, is the seminal difference between the Cosserat and the classic continuum mechanics. Equation 10 shows that for l approaching zero, and therefore B also approaching zero, from the last expression of Equation 9, it can be seen that the moment stresses tend to vanish.

There are many proposals for working with elastoplasticity in a Cosserat continuum (e.g., Lippmann, 1969; Besdo, 1985; Bogardanova-Bontcheva & Lippmann, 1975; Vardoulakis & Sulem, 1995). The one implemented in the numerical models presented below is a modification of Bogdanova-Bontcheva & Lippmann (1975) proposed by Figueiredo (1999). Specifically, flow criteria f and plastic potential functions g are formulated for the instauration of mechanical instability for shear, for the moment stresses and for the rotation of the microstructure with a characteristic length l. Thus, analogously to the Mohr-Coulomb criterion, one can write:

$$f_1 = \sqrt{J_2} + I_1^e \sin \varnothing + (|\sigma^a| - \sigma_0) \cos \varnothing$$
$$g_1 = \sqrt{J_2} + I_1^e \sin\psi + (|\sigma^a| - \sigma_0) \cos\psi \qquad (11)$$

where J_2 is the second invariant of the symmetric part of the Cosserat deviatoric stress tensor, I_1^e is the first invariant of the Cosserat effective stress tensor, σ_0 is the cohesion, ϕ is the internal friction angle and ψ is the angle of dilatancy. The flow criterion involving the moment stresses is given by:

$$f_2 = \sqrt{J_2^m} - \sigma_0 l$$
$$g_2 = f_2 \qquad (12)$$

where J_2^m is the second invariant of the symmetric part of the deviatoric moment stresses tensor. In its turn, the flow criterion for the rotation of the microstructure, originally proposed by Figueiredo (1999), is written as:

$$f_3 = |m\text{-}2\sigma^a l| + \sigma_N{}^{ec}\left(\frac{l \tan \phi_r}{2}\right) - \sigma_0 l$$
$$g_3 = f_3 \qquad (13)$$

where σ_N^{ec} is the Cosserat effective normal stress acting in the plane of rupture and ϕ_r is the rotational friction angle, to be defined below.

3 Modelling Geologic Materials as Cosserat Generalized Continuum Media

The mechanics of Cosserat generalized continuum allows broadening the interpretation and implications of structural models for rocks. In fact, its core characteristics as formulation with characteristic lengths of the medium, the possibility of microstructure rotations as an independent field from macroscale and the establishment of tensor asymmetry can cast another light in structural geology modelling. In this sense, it will be suggested some simple but illustrative examples based upon conceptual, analytical and numerical arguments.

As shown in Figueiredo *et al*. (2004), the properties of Mohr diagrams in 2D classic continuum can be extended to a Cosserat continuum. In their parametric form, the equations for the Cosserat normal σ^c_N and Cosserat shear σ^c_C stresses in a plane can be written as a function of the angle θ between the maximum principal stress and the plane as:

$$\sigma^c{}_N = \frac{(\sigma^c_{11}+\sigma^c_{22})}{2} - \frac{(\sigma^c_{11}-\sigma^c_{22})}{2}\cos 2\theta + \frac{(\sigma^c_{12}+\sigma^c_{21})}{2}\sin 2\theta$$
$$\sigma^c{}_C = \sigma^a + \frac{(\sigma^c_{11}-\sigma^c_{22})}{2}\sin 2\theta + \frac{(\sigma^c_{12}+\sigma^c_{21})}{2}\cos 2\theta \qquad (14)$$

Note that the anti-symmetric shear stress, given by Equation 8, appears in the expression for the Cosserat shear stress. As such, Equation 14 implies, as shown in Figure 2, that the shear stresses of the classic continuum are "displaced" in the σ^c_N x σ^c_C space along the shear stress axis by a amount σ^a. An immediate consequence is that the principal stresses (i.e. those acting on planes where σ^c_C vanishes) should not be orthogonal as in the classic continuum and, depending on the value of σ^a, could even no longer exist. Taking these stress and strain equivalent frameworks, as at some extent already pointed by De Paor (1994), one can suggest that the asymmetric structuring patterns in shear zones may perhaps be better compatibilized by using the mechanics of Cosserat generalized continuum. In fact, as synthesized in Simpson & De Paor (1993), shear zones bear strain non-coaxial fields, vorticity complexes fields and non-orthogonal strain rates eigenvectors for defining the apophyses, elements not yet satisfactorily explained by the classic continuum mechanics. In this sense, it could be possible to extend expressions relating stresses and strains in shear zones in a more cause-consequence fashion.

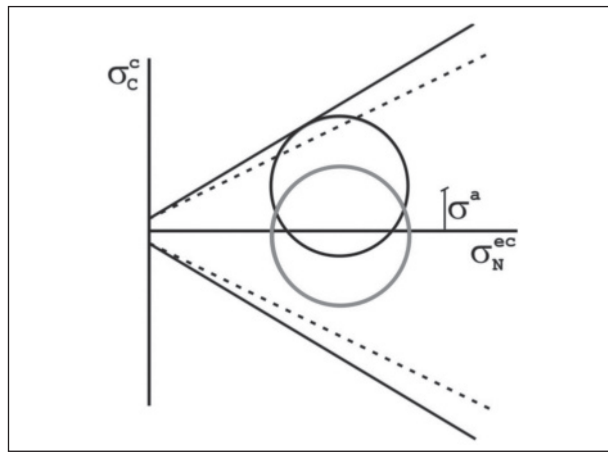

Figure 2 Mohr diagram in 2D showing as shear stresses are "displaced" in the σ^{ec}_N x σ^c_C space along the shear stress axis by a amount σ^a, the anti-symmetric shear stress. Stress state for the classic continuum in gray and for Cosserat continuum in black. Flow criteria for shear in full line and for rotation in dashed line. In this case, there is a combined effect of rotation and sliding as both envelopes are reached by the stress state.

In addition, considering the failure envelopes analogous to Equation 11 and Equation 13 in the space σ^{ec}_N x σ^c_C, Figure 2 suggests how the asymmetry of the Cosserat stress tensor may favour the emergence of fault zones with a single orientation and not as conjugated structures. In this case, there would be a combination of rotation of the microstructure and sliding as the two envelopes are touched by the Cosserat stress state. Indeed, in nature fault zones appear less frequently as conjugate and symmetric structures. An inspection of several seismic sections and analogue physical models, for example as shown in Jackson & Hudec (2017), suggests that the most expressive faults have rough parallel geometry and hardly appear as sistematic conjugated faults.

The spatial arrangement of the microstructures in rocks, coming from either the geometry of single mineral grains or of their associations due to the stress loading conditions forming chains of mineral grains, may determine the rock strength. Similar to what was performed by Nascimento & Teixeira (1971), Figure 3 represents an allegory illustrating the impact of the structure geometry on the study of the mechanical stability in any material. Ultimately it is the classic slope plane-block problem in which the conservation of linear and angular moments for the block is analyzed by regarding the weight, normal and friction forces. Considering a the height and b the base of a block with mass m and g the acceleration due to gravity, for the case in Figure 3a it is known that in the limit for block sliding (slope α):

$$mg\sin\alpha - \mu_e mg\cos\alpha = 0 \Rightarrow \tan\alpha = \mu_e \Rightarrow \phi_e = \alpha \quad (15)$$

where μ_e is the static friction coefficient and ϕ_e is the static friction angle. In this case, the base of the block has a length greater than its height, so that it can slide without rolling when the plane reaches the angle α corresponding to the sliding condition. The resulting torque is zero as the torque due to the weight force is balanced by the torque due to the contact forces (normal and friction forces). On the other hand, in Figure 3b the base of the block has a length smaller than its height. Assuming that ϕ_e is high enough to prevent sliping, the torque due to the weight calculated relatively to the lower right corner of the block for the toppling limit condition (slope β) is given by:

$$mg\sin\beta(a/2) - mg\cos\beta(b/2) = 0 \Rightarrow \tan\beta = \left(\frac{b}{a}\right) \Rightarrow \phi_r = \beta \Rightarrow \phi_r = \arctan\left(\frac{b}{a}\right) \quad (15)$$

where ϕ_r is the rotational friction angle. In words, the occurrence or not of block rotation is dramatically dependent on the relationship between its geometry and the load distribution. When $b > a$ we have $\beta > \alpha$ and $\phi_r > \phi_e$, what would cause the block to slip. Otherwise, when $b < a$ we have $\beta < \alpha$ and $\phi_r < \phi_e$, what could lead the block to rotate.

Although this allegory is quite naive at a first glance, its mechanical context can be heuristically extend to what occurs to rocks. Figure 4 shows the loading condition in a set of blocks representing the inner microstructures in rocks. Note that the base and height ratios for the blocks are inverse in Figs. 4a and 4b. Thus, though the shear strength criteria is the same for both the rotation criteria are different. For the sake of an example, it is assumed that $\sigma^c_{11} = \sigma^c_{22}$ and $\sigma^c_{21} > \sigma^c_{12}$, implying a negative anti-symmetric shear stress σ^a in both cases, in according to Equation 8, and f_r is greater in Figure 4a than in Figure 4b, in according to Equation 16. Note that the difference between σ^c_{21} and σ^c_{12} is balanced by the emergence of moment stresses according to the last expression of Equation 7. After imposing the load condition, the Mohr diagrams show only shearing in the sub-horizontal direction in the basal contacts among the blocks in Figure 4a and clockwise rotation of the blocks and later shearing in the contacts among the blocks in Figure 4b. It is very suggestive that the rotation patterns and relative shearing of the microstructures in the rock could explain, for example, the sinthetic Y, R and P and the antithetic R' and X structures of the classic Riedel-Tchalenko experiment, favoring one to other in the progress of deformation. Regarding the specific conditions in Figure 4, we could postulate the onset of Y structures in Figure 4a and, due to the clockwise rotation of the blocks, of R' or even of X structures (depending on the amount of rotation) and of Y structures in Figure 4b. Of course, a paramount of scenarios may arise depending on the stresses conditions and the spatial arrangement of the microstructure in rocks.

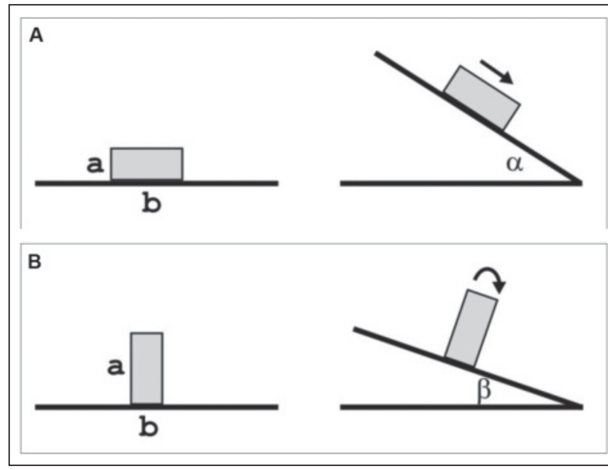

Figure 3 Impact of block geometry in the analysis of its stability in the classic slope plane-block system problem. Different aspect ratios between block base b and height a determine if the block slides or topples. Considering Equation 16, in (a) as $b > a$ and $\phi_r > \phi$ the block could slide without toppling; in (b) as $b < a$ and $\phi_r < \phi$ block could topples before sliding.

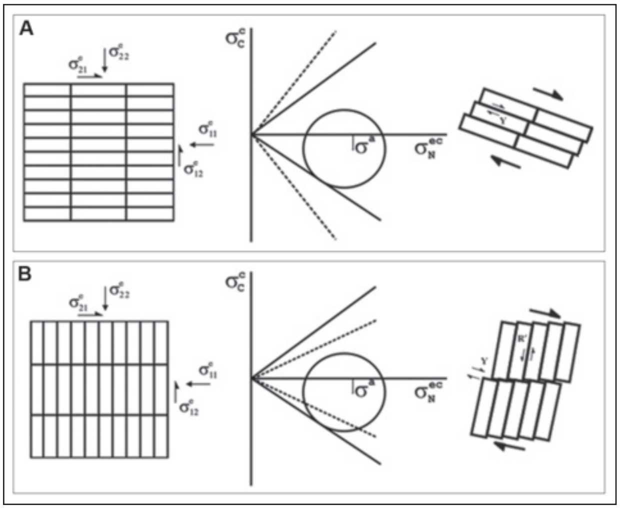

Figure 4 Loading in sets of blocks representing the inner microstructure in rocks. Shear strength criteria (full line) is the same in (a) and (b) whereas the base and height ratios for the blocks are inverse in (a) and (b) the rotation criteria (dashed line) are also different. As an example, with $\sigma^c_{11} = \sigma^c_{22}$ and $\sigma^c_{21} > \sigma^c_{12}$, σ^a is negative, in according to Equation 8, and ϕ_r is greater in (a) than in (b), in according to Equation 16. Mohr diagrams and deformed configuration show shearing in the basal contacts among the blocks in (a) and clockwise rotation of the blocks and shearing in the basal contacts among the blocks in (b).

From what was pointed out, it is suggestive that the relation between the spatial arrangement of the rock structure and the normal and shear stresses that it can support depends not only on the analysis of the slip conditions but also on the analysis of the microstructure rotation conditions. Regarding the internal friction angle of rocks as the fundamental concept related to their strength, although without intending to offer a physical interpretation for it (as it is an empirical parameter), we can do some digressions. The basic one is that the internal friction angle could be weighted either by the static friction angle and by the rotational friction angle depending on the spatial distribution of the rock structure in relation to the stresses. In this context, the formulation of the mechanics of Cosserat generalized continuum should be very important in assessing the role of microstructure rotation in what is classically called internal friction coefficient for rocks.

Pristine rock fabric can readily be expressed by the characteristic lengths in the formulation of the mechanics of Cosserat generalized continuum. In order to assess the role of the characteristic length in the inner structure of fault zones, some numerical models were conducted by using the computer system TECTOS, a finite-element based system developed by Petrobras and the Catholic University of Rio de Janeiro (Moraes *et al.*, 2002). Figure 5 provides the geometry, the mesh and the boundary conditions for the models. They have a non-associated elastoplastic rheology with an internal friction angle of 30∈ and a dilatancy angle of 12∈. A rotational modulus G_r of 25 GPa was used as well as isotropic characteristic lengths l of 0.01 m, 0.1 m, 1 m, 2.5 m and 10 m. Further properties as well the boundary conditions are suitable for the conditions at a depth of 5 km in the crust. A progressive dextral shear stress from 10 to 90 MPa was prescribed at the top and the bottom of the models. Figure 6 shows the results for rupture and the anti-symmetric shear stress at the latter stage for the models. A model for the classic continuum is also shown for comparison. Here, the concept of anti-symmetric shear stress rigorously does not apply, being basically zero. Comparing the failure patterns in the models, it is seen that the model carried by the classic continuum mechanics shows a generalized rupture in the fault zone. In contrast, the models governed by the mechanics of Cosserat generalized continuum show a strong banded pattern for the strain localization, with intercalation of sub-parallel strands with and without rupture that are in general proportional to the characteristic lengths. These results suggest a consistent spatial complexity in the onset of faulting not captured by the the classic continuum mechanics model. By observing the anti-symmetric shear stresses, negative values for clockwise rotations, the role of the characteristic length in structuring a fault zone becomes clear. The complexity in terms of microscale rotation fields, with heterogeneous clockwise and counter-clockwise distribution, is larger for smaller characteristic lengths and less pronouced for larger characteristic lengths. As previously stated, fault structural fabric, specially Riedel-Tchalenko structures with their sinthetic or antithetic shearing patterns, could be a consequence of the heterogeneous moment stresses field along the fault zone. In a broad sense, the results of the numerical models suggest that models using the mechanics of Cosserat generalized continuum bear a greater appeal to discuss the inner organization of fault zones in terms of rupture pattern and generation of their asymmetric fabric.

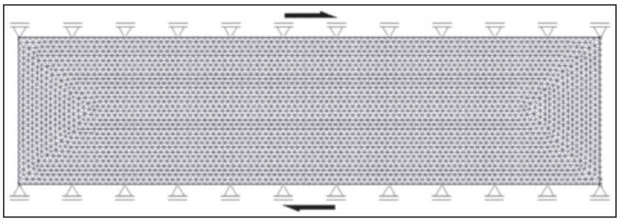

Figure 5 Geometry, mesh and boundary conditions for the finite-element models. The models have 25 m by 100 m and a non-structured mesh. Boundary conditions are suitable for a depth of 5 km in the crust. A progressive dextral shear from 10 to 90 MPa was prescribed at the top and the bottom of the models.

In this way, we postulate that the discussion on the spatial arrangement of the fabric in fault zones is rarely extended as most of the works in fault zones modelling usually makes use of the classic continuum mechanics. For example, many authors in the structural geology literature endeavour to explain the very common antithetic features relying only on classic continuum mechanics. Ramsay (1967), page 283, points out the need to have a "*disequilibrium component*" in the stress tensor as "*the disequilibrium components cause the material to undergo a rotation in space*". In fact, this component need not to exist as the relative stress tensor t_{ij}, the anti-symmetric part of the Cosserat stress tensor, leads to anti-symmetric shear stresses and related rotations. Mandl (1999) recognizes the need for the emergence of antithetic features when studying many structural and geodynamic problems (e.g. antithetic faults, bookshelf mechanism, San Andreas Fault Paradox). However, the author follows a complex path for the explanation of these geodynamic contexts by making several transformations in the space σ^e_N x σ_C together with the Mohr-Coulomb criterion. Nevertheless, by using the mechanics of Cosserat generalized continuum, many antithetic features may easily emerge. Ahlgren (2001) places R' structures as "*enigmatic features*" and considers that "*the antithetic shear sense of these bands ... is difficult to interpret mechanically*". Once again, the presence of the anti-symmetric shear stresses could provide an adequate interpretation.

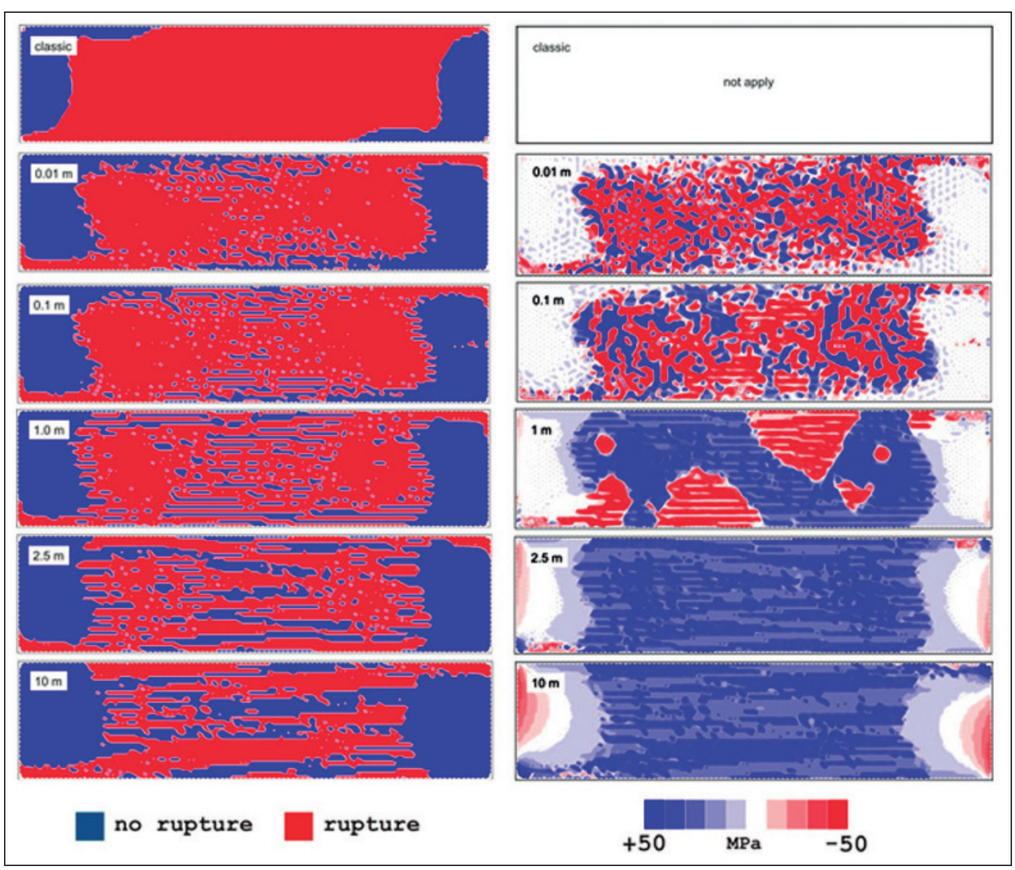

Figure 6 Results of the numerical models for a classic continuum and for some Cosserat continua with different characteristic lengths of 0.01 m, 0.1 m, 1 m, 2.5 m and 10 m; (a) rupture; (b) anti-symmetric shear stresses (negative values for clockwise rotations).

4 Concluding Remarks

It is suggestive that asymmetric geological structures are generated by asymmetric physical fields. According to what was discussed, we ponder that the mechanics of Cosserat generalized continuum allow a better comprehension when building and interpreting conceptual and, in special, numerical models in structural geology. In a broad sense, in comparison to the classic continuum mechanics, the mechanics of Cosserat generalized continuum deals more widely with heterogeneous and anisotropic media, that is, the seminal characteristics present in rocks. In this sense, we argue that by using the Cosserat continuum mechanics it would be possible to better define the observation scales to be considered in defining how heterogeneous is the deformation responsible for the structural symmetry/asymmetry in rocks.

Considering future perspectives, it would be of fundamental importance to develop more refined models based on the intrinsic formulation of a Cosserat's continuum and to extend its relationship with the experimental base and the observations in nature. In particular, it would be very useful to characterize the role of the characteristic lengths either in isotropic or in anisotropic rocks and their physical meaning and relevance in studying any particular set of geological structures.

5 Ackowledgements

Anderson Moraes is grateful to Petrobras for allowing to publish this work. We thank two anonymous reviewers who greatly helped to improve the manuscript.

6 References

Adhikary, D.P.; Mühlhaus, H.B. & Dyskin, A.V. 1999. Modelling the Large Deformations in Stratified Media - the Cosserat Continuum Approach. *Mechanics of Cohesive-frictional Materials*, 4:195-213.

Ahlgren, S.G. 2001. The Nucleation and Evolution of Riedel Shear Zones as Deformation Bands in Porous Sandstones. *Journal of Structural Geology*, 23:1203-1214.

Bauer, E. & Tejchman, J. 1995. Numerical Study of the Effect of Grain Rotations on Material Behavior in a Fault Zone. *In*: ROSSMANITH, A. (ed.). *Mechanics of Jointed and Faulted Rock*. Balkema, p.317-322.

Besdo, D. 1985. Inelastic Behaviour of Plane Frictionless Block-Systems Described as Cosserat Media. *Archives of Mechanics*, 37:603-619.

Bigoni, D. & Gourgiotis, P.A. 2016. Folding and Faulting of an Elastic Continuum. *Proceedings of the Royal Society*, A472:20160018.

Biot, M.A. 1965. *Mechanics of Incremental Deformations*. Nova Iorque, John Wiley and Sons, 504p.

Biot, M.A. 1967. Rheological Stability with Couple-Stresses and Its Applications to Geological Folding. *Proceedings of the Royal Society of London*, A2298:402-423.

Bogdanova-Bontcheva, N. & Lippmann, H. 1975. Rotationssymmetrisches Ebenes Flißen Eines Granularen Modellmaterials. *Acta Mechanica*, 21:93-113.

Coetzee, C.J. 2014. Discrete and Continuum Modelling of Soil Cutting. *Computational Particle Mechanics*, 4:409-423.

Cosserat, E. & Cosserat, F. 1909. *Théorie des Corps D*éformables. Paris, Hermann et Fils, 226p.

De Paor, D.G. 1994. The Role of Asymmetry in the Formation of Structures. *Journal of Structural Geology*, 4:467-475.

Esin, M.; Dyskin, A.V.; Pasternak, E. & Xu, Y., 2017. Mode I Crack in Particulate Materials with Rotational Degrees of Freedom. *Engineering Fracture Mechanics*, 172:181-195.

Figueiredo, R.P. 1999. Modelagem de Maciços Rochosos como Meios Contínuos Generalizados de Cosserat. Pontifícia Universidade Católica do Rio de Janeiro, Tese de Doutorado, 249p.

Figueiredo, R.P.; Vargas, E.A. & Moraes, A. 2004. Analysis of Bookshelf Mechanisms Using the Mechanics of Cosserat Generalized Continua. *Journal of Structural Geology*, 26:1931-1943.

Germain, P. 1973. La Méthode des Puissances Virtuelles en Mécanique des Milieux Continus. Première Partie: Théorie du Second Gradient. *Journal de Mécanique*, 12:235-274.

Jackson, M.P.A. & Hudec, M.R. 2017. *Salt Tectonics. Principles and Practice*. Nova Iorque, Cambridge University Press, 498p.

Khoei, A.R.; Yadegari, S. & Biabanaki, S.O.R. 2010. 3D Finite Element Modeling of Shear Band Localization Via the Micro-polar Cosserat Continuum Theory. *Computational Materials Science*, 49:720-733.

Latham, J.P. 1985a. The Influence of Nonlinear Materials Properties and Resistance to Bending on the Development of Internal Structures. *Journal of Structural Geology*, 7:225-236.

Latham, J.P. 1985b. A Numerical Investigation and Geological Discussion of the Relationship Between Folding, Kinking and Fracturing. *Journal of Structural Geology*, 7:237-249.

Lee, W.H.K. 2011. Rotational Seismology. *In*: GUPTA, H.K. (ed.). *Encyclopedia of Solid Earth Geophysic*. Springer, p.1344-1355.

Lippmann, H. 1969. Eine Cosserat-Theorie das Plastischen Flißens. *Acta Mechanica*, 8:255-284.

Mandl, G. 1999. *Faulting in Brittle Rocks*. Berlim, Elsevier, 434p.

Maugin, G.A. 2017. *Non-Classical Continuum Mechanics. A Dictionary*. Singapura, Springer, 259p.

Mindlin, R.D. 1963. Influence of Couple-Stress on Stress Concentrations. *Experimental Mechanics*, 3:1-7.

Moraes, A. 2004. Comportamento Mecânico de Zonas de Falhas. Universidade Federal do Rio de Janeiro, Tese de Doutorado, 300p.

Moraes, A.; Conceição, J.C.J.; Campos, J.L.; Vargas Jr, E.A. 2002. TECTOS: Programa de Modelagem Mecânica em Geologia Estrutural. *In*: Congresso Brasileiro de Geologia, 41, João Pessoa, 2002. Resumos, João Pessoa, SBG, p.627.

Mühlhaus, H.B. & Vardoulakis, I.G. 1987. The Thickness of Shear Bands in Granular Materials. *Géotechnique*, 37: 271-283.

Mühlhaus, H.B.; Dufour, F.; Moresi, L. & Hobbs, B. 2002. A Director Theory for Visco-Elastic Folding Instabilities in Multilayered Rock. *International Journal of Solids and Structures*, 39:3675-3691.

Muller, A.L.; Vargas, E.A.; Vaz, L.E.; Figueiredo, R.P. & Gonçalves, C.J. 2011. Numerical Analysis of Sand/Solids Production in Boreholes Considering Fluid-Mechanical Coupling in a Cosserat Continuum. *International Journal of Rock Mechanics and Mining Sciences*, 48:1303-1312.

Nascimento, U. & Teixeira, H. 1971. Mechanisms of Internal Friction in Soils and Rocks. *In*: SOCIETY OF ROCK MECHANICS SYMPOSIUM, Nancy, 1971, II-3.

Ostoja-Starzewski, M.; Li, J. & Demmie, P.N. 2019. Continuum Homogenization of Fractal Media. *In*: VOYIADJIS, G.Z. (ed.). *Handbook of Nonlocal Continuum Mechanics for Materials and Structures*. Springer, p.905-935.

Ramsay, J.G. 1967. *Folding and Fracturing of Rocks*. Nova Iorque, McGraw-Hill, 568p.

Rattez, H.; Stefanou, I.; Sulem, J.; Veveakis, M. & Poulet, T. 2018. Numerical Analysis of Strain Localization in Rocks with Thermo-Hydro-Mechanical Couplings Using Cosserat Continuum. *Rock Mechanics and Rock Engineering*, 51:3295-3311.

Simpson, C. & De Paor, D.G. 1993. Strain and Kinematic Analysis in General Shear Zones. *Journal of Structural Geology*, 15:1-20.

Sternberg, E. & Muki, R. 1967. The Effects of Couple-Stress on the Stress Concentration Around a Crack. *International Journal of Solids and Structures*, 3:69-95.

Teisseyre, R. 2012. Asymmetric Continuum Theories. Fracture Processes in Seismology and Extreme Fluid Dynamics. *In*: LIM, H.S. (ed.). *New Achievements in Geoscience*. InTech, p.199-212.

Tejchman, J. 2008. *Shear Localization in Granular Bodies with Micro-Polar Hypoplasticity*. Berlim, Springer.

Teodorescu, P.P. 1975. *Dynamics of Linear Elastic Bodies*. Bucareste, Editura Academiei.

Tordesillas, A.; Peters, J.F. & Gardiner, B.S. 2004. Shear Band Evolution and Accumulated Microstructural Development in Cosserat Media. *International Journal for Numerical and Analytical Methods in Geomechanics*, 28:981-1010.

Twiss, R.J.; Protzman, G.M. & Hurst, S.D. 1991. Theory of Slickenline Patterns Based on the Velocity Gradient Tensor and Microrotation. *Tectonophysics*, 186:215-239.

Twiss, R.J.; Souter, B.J. & Unruh, J.R. 1993. The Effect of Block Rotations on the Global Seismic Moment Tensor and the Patterns os Seismic P and T Axes. *Journal of Geophysical Research: Solid Earth*, 98:645-674.

Twiss, R.J. & Unruh, J.R. 1998. Analysis of Fault Slip Inversions: Do They Constrain Stress or Strain Rate? *Journal of Geophysical Research: Solid Earth*, 103:12205-12222.

Twiss, R.J. & Unruh, J.R. 2007. Structure, Deformation, and Strength of the Loma Prieta Fault, Northern California, USA, as Inferred From the 1989-1990 Loma Prieta Aftershock Sequence. *Geological Society of America Bulletin*, 119:1079-1106.

Vardoulakis, I.G. & Sulem, J., 1995. *Bifurcation Analysis in Geomechanics*. Londres, Chapman Hall, 447p.

Veveakis, E.; Sulem, J. & Stefanou, I. 2012. Modeling of Fault Gouges with Cosserat Continuum Mechanics: Influence of Thermal Pressurization and Chemical Decomposition as Coseismic Weakening Mechanisms, *Journal of Structural Geology*, 38:254-264.

Žalohar, J. & Vrabec, M. 2010. Kinematics and Dynamics of Fault Reactivation: the Cosserat Approach. *Journal of Structural Geology*, 32:15-27.

Žalohar, J. 2012. Cosserat Analysis of Interactions Between Intersecting Faults; the Wedge Faulting. *Journal of Structural Geology*, 37:105-123.

Žalohar, J. 2014. Explaining the Physical Origin of Båth´s Law. *Journal of Structural Geology*, 60:30-45.

Žalohar, J. 2015. On a New Law of Faulting Along Tectonic Wedges: Cosserat Explanation of the Preferred (Paleo) Stress States in the Earth´s Crust. *Journal of Structural Geology*, 77:107-125.

Žalohar, J. 2018. The Omega-Theory. A New Physics of Earthquakes. Amsterdam, Elsevier, 570p.

Zheng, Z.; Sun, W. & Fish, J. 2016. Micropolar Effect on the Cataclastic Flow and Brittle-Ductile Transition in High-Porosity Rocks. *Journal of Geophysical Research: Solid Earth*, 121: 1425-1440.